A corner transfer matrix renormalization group investigation of the vertex-interacting self-avoiding walk model

2003 J. Phys. A: Math. Gen. 36 10279

(http://iopscience.iop.org/0305-4470/36/41/003)

INSTITUTE OF PHYSICS PUBLISHING JOURNAL OF PHYSICS A: MATHEMATICAL AND GENERAL

J. Phys. A: Math. Gen. **36** (2003) 10279–10298 PII: S0305-4470(03)66209-8

A corner transfer matrix renormalization group investigation of the vertex-interacting self-avoiding walk model

D P Foster and C Pinettes

Laboratoire de Physique Théorique et Modélisation (CNRS UMR 8089), Université de Cergy-Pontoise, 5 Mail Gay-Lussac 95031, Cergy-Pontoise Cedex, France

Received 17 July 2003
Published 1 October 2003
Online at stacks.iop.org/JPhysA/36/10279

Abstract

A recently introduced extension of the corner transfer matrix renormalization group method useful for the study of self-avoiding walk-type models is presented in detail and applied to a class of interacting self-avoiding walks due to Blöte and Nienhuis. This model displays two different types of collapse transition depending on model parameters. One is the standard θ-point transition. The other is found to give rise to a first-order collapse transition despite being known to be in other respects critical.

PACS numbers: 36.20.−r, 64.60.−i

1. Introduction

Self-avoiding walk models are of interest as models of polymers in solution [1] as well as realizations of $O(n)$ spin models in the limit $n \to 0$ [2].

The self-avoiding walk problem is a difficult problem numerically because of the intrinsic long-ranged nature of the problem; self-avoiding walks are extended objects. The numerical methods most used to date for the study of such models are Monte Carlo simulations [3], series expansions [4] and transfer matrix calculations [5–10].

Monte Carlo simulations are hampered by problems of trapping in the low temperature, or equivalently large interaction, phases. These may be relieved using the fluctuating bond method [3, 11], which also enables the investigation of the dense-walk phases. This method has the drawback of modifying the model in a way which is not always convenient, particularly if frustration effects are of interest. Current Monte Carlo methods, such as the PERM method [12] and parallel tempering [13], relieve these difficulties to some extent, but at the cost of computational complexity.

Series expansions are limited by the lengths of walks that may be enumerated. In practice these are limited to a few tens of lattice steps. Very technical methods may be used to achieve longer series expansions of the partition function (of the order of 60 lattice steps), and in some

cases the estimate of the critical point is very impressive [14]. If correlation length exponents are required, then the range of walk lengths open to enumeration are of the order of 30 steps [15]. This becomes increasingly limiting as the complexity of the model increases.

Transfer matrices have the advantage over Monte Carlo simulations of giving numerically exact values of the free energy, correlation lengths, polymer densities,etc, for strips of infinite length, but of finite width. Finite-size analysis methods then allow the extrapolation of the finite-size estimates. The widths of lattice accessible are limited: for the self-avoiding walk model widths up to 12 or 14 are possible (see for example [16]), but this again drops as the complexity of the model increases (see for example [17]). It often occurs that the number of data points one may use in finite-size analysis becomes dangerously small for finite-size scaling techniques to be of use, particularly if odd/even parity effects are present.

In this paper, we apply a recent extension of the corner transfer matrix renormalization group (CTMRG) method [18] to a class of self-avoiding walks introduced by Blöte and Nienhuis, which we shall refer to as the vertex-interacting self-avoiding walk model, to reflect the fact that the monomer–monomer interactions are added for doubly visited sites (for a full description of the model see section 2.1). We will show that the CTMRG method extends the possibilities of transfer matrices to larger system sizes, at the cost of introducing a phase space truncation scheme. The accuracy of the results is however controllable through a parameter m corresponding to the number of states kept from one iteration to the next.

The other important result in this paper relates to the vertex-interacting self-avoiding walk model. Whilst it has the standard collapse transition as a special case (where the walk is obliged to turn after each step), it is believed to have a generic collapse transition in a different universality class [16]. We show that this collapse transition has a first-order character, despite the fact that there exists critical exponent $\nu = 12/23$ which has been exactly determined by Warnaar *et al* [19].

2. The corner transfer matrix renormalization method

Transfer matrices, as a numerical method, have a major advantage over Monte Carlo methods in that they sum over all possible configurations, and so are not hampered by trapping effects at low temperatures (or high densities in polymer problems) which plague Monte Carlo simulations of models with competing interactions (frustrated models).

The major inconvenience is the large amount of computer memory required to store the matrices, limiting the maximum lattice width in practical calculations. This is alleviated in part by finite-size analysis methods which work well [20], at least for the simpler models, coupled with efficient extrapolation methods [21].

In two-dimensional classical spin models, or one-dimensional quantum spin models, there exist iterative approximation schemes which, by successive pruning of phase space, permit calculations for much larger lattice widths for given computer resources. These methods are the density matrix renormalization group method (DMRG) [22, 23] and the corner transfer matrix renormalization group method (CTMRG) [24]. These methods have little recourse to the renormalization group, and are better thought of as iterative matrix approximation schemes. The basic idea is that the (approximate) transfer matrix for a lattice of size $2N$ is calculated from the transfer matrix for a lattice of size $2N - 2$ by inserting extra lattice sites. A change of basis is then performed, such that the transfer matrix may be projected onto a smaller basis, with the smallest possible loss of information.

In a recent paper we showed how the CTMRG method, first introduced for classical spin systems by Nishino [24], may be applied to self-avoiding walk-type models [18]. This requires a non-trivial modification of the method since the iteration scheme requires all interactions

to be local. The self-walk problem, by its very nature, is non-local. In the remainder of this section the details of the method, absent in [18], are provided. In particular we show how this non-locality may be overcome, and describe the implementation of CTMRG for this class of problem.

2.1. The self-avoiding walk, the $O(n)$ model and vertex models with complex weights

It is known that spin models with $O(n)$ invariant spins have high-temperature expansions consisting of closed loops. The self-avoiding loop (SAL) model is related to the high-temperature expansion of the $O(n = 0)$ model [2]. In a similar way, the high-temperature expansion of the susceptibility leads to a model with one open path, and a gas of loops [25]. The $n \to 0$ limit eliminates the loops to leave a self-avoiding walk. The partition function for a self-avoiding walk is thus equivalent to the susceptibility of an $O(n = 0)$ spin model.

The connection between the $O(n)$ class of models and better known models is as follows: $n = 1$ corresponds to the Ising model, $n = 2$ to the XY model and $n = 3$ to the classical Heisenberg model. The partition functions of these models are given by

$$\mathcal{Z} = \sum_{\{\vec{s}_i\}} \exp\left(\frac{1}{2}\beta J \sum_{\langle i,j\rangle} \vec{s}_i \cdot \vec{s}_j\right) \tag{1}$$

where $\langle i, j\rangle$ refers to a sum over nearest-neighbour spins. Whilst the high-temperature expansion of the Ising model is relatively easy, the expansion for other values of n is a little cumbersome. In what follows we shall consider a slightly different $O(n)$ invariant model, due to Nienhuis [26, 27], with the partition function given by

$$\mathcal{Z}_{O(n)} = \sum_{\{s_i^\alpha\}} \prod_{\langle i,j\rangle} \left(1 + K \sum_{\alpha=1}^{n} s_i^\alpha s_j^\alpha\right) \tag{2}$$

where the spins, $s_i^\alpha = \pm 1$, are placed on the lattice bonds. A diagrammatic expansion of equation (2) follows if we identify the 1 as the weight of an empty bond between the sites i and j and the K as the weight of an occupied bond. Since $\langle s_i^\alpha \rangle = 0$ and $\left(s_i^\alpha\right)^2 = 1$, the only terms in the expansion of equation (2) which survive the sum over $\left\{s_i^\alpha\right\}$ are those terms consisting of closed loops where the 'colour' α is conserved around each loop. Different loops may have different 'colours'. The sum over α gives a factor n for each loop. An equivalent expression for equation (2) may now be given in terms of loop graphs $\mathcal{G}$:

$$\mathcal{Z}_{O(n)} = \sum_{\mathcal{G}} n^{l(\mathcal{G})} K^{b(\mathcal{G})} \tag{3}$$

where l is the number of loops and b is the number of occupied bonds. The partition for self-avoiding loops is then just

$$\mathcal{Z}_{\mathrm{SAL}} = \lim_{n\to 0} \frac{1}{n} \mathcal{Z}_{O(n)}. \tag{4}$$

The parameter n is now a fugacity controlling the number of loops, and in this representation need no longer be taken as an integer. This fugacity corresponds to a long-range interaction, since the loops may be of any size. This non-locality is undesirable for our purposes. We would like to express n as a product over local weights despite the variable size of the loops. The only real numbers with this property are 0 and 1. This leads us to introduce complex local weights, w_i. If $|w_i| = 1$, the product of the w_i around a loop will also be of modulus 1. The final weight must, however, be real. This may be achieved if for every complex weight, we also have its complex conjugate. Each loop may be followed clockwise or

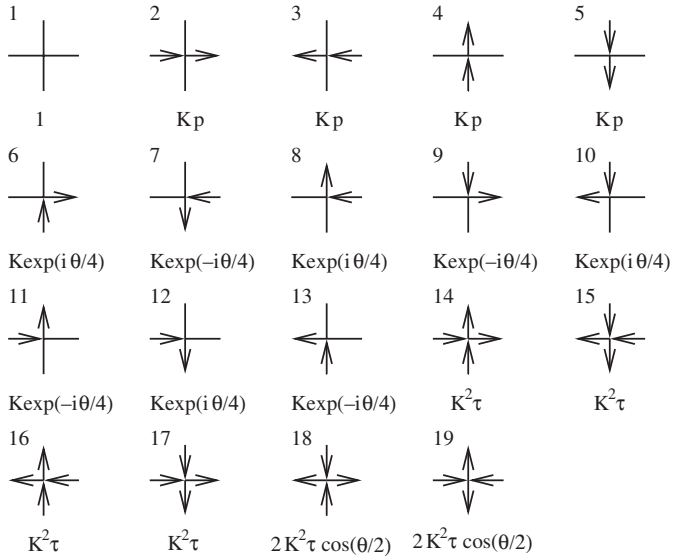

Figure 1. The 19 allowed vertices in the Nienhuis $O(n)$ class of models, with the weights for the vertex-interacting self-avoiding walk model ($\theta = \pi/2$). K is the step fugacity and $\tau = \exp(-\beta\varepsilon)$ is the Boltzmann weight associated with non-intersecting site interactions.

anticlockwise. The loops in equation (3) are not oriented, but may be oriented by associating $2^{l(\mathcal{G})}$ oriented graphs with each non-oriented graph. The loop fugacity is not required to be the same for the two orientations of the loop, and so a fugacity n_+ (n_-) is associated with (anti)clockwise oriented loops. The partition function may then be written as [26, 27]

$$\mathcal{Z}_{O(n)} = \sum_{\mathcal{G}} (n_+ + n_-)^l K^b \tag{5}$$

$$= \sum_{\mathcal{G}'} n_+^{l_+} n_-^{l_-} K^b \tag{6}$$

where $\mathcal{G}'$ is the set of oriented loop graphs and l_+ (l_-) is the number of (anti)clockwise oriented loops. On the square lattice there must be four more corners with one orientation, compared to the other orientation, in order to close a loop. Using this fact we may set $w_i = \exp(\mathrm{i}\theta/4)$ for a clockwise corner, $w_i = \exp(-\mathrm{i}\theta/4)$ for an anticlockwise corner and $w_i = 1$ otherwise. This leads to $n_+ = \exp(\mathrm{i}\theta)$ and $n_- = \exp(-\mathrm{i}\theta)$, and hence $n = 2\cos(\theta)$. The oriented loop factor has now been broken up into local weights and the partition function may be rewritten in terms of a vertex model [28, 29]:

$$\mathcal{Z} = \sum_{\mathcal{G}'} \prod_i v_i \tag{7}$$

where v_i is the weight of the vertex found at site i. The possible vertices are shown in figure 1. The derivation given here is only for the simplest case, but we may freely change the weights of the vertex configurations in order to generate different interactions in the original model. Notably, to have exactly the standard self-avoiding walk model it is necessary to set the weights of vertices 14 to 19 to zero, and set $n = 0$, or equivalently set $\theta = \pi/2$.

A vertex model may be thought of as a spin model where the spins live on the bonds of the lattice. Each spin has three states corresponding to the empty lattice bond, a bond

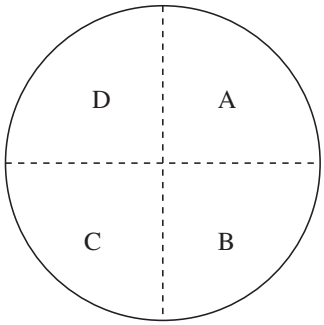

Figure 2. A schematic representation of the two-dimensional lattice split into four quarters, represented by the four corner matrices **A, B, C** and **D**.

oriented in the positive x (y) direction and a bond oriented in the negative x (y) direction. The vertex weights may be written as a vertex function $W(\sigma_i, \sigma_j, \sigma_k, \sigma_l)$, where the tensor elements correspond to the vertex weights of figure 1. The vertex function was defined using the following convention:

$$\sigma = \begin{cases} 1 & \text{if the bond has an arrow to the right or upwards} \\ 0 & \text{if the bond has no arrow} \\ -1 & \text{if the bond has an arrow to the left or down.} \end{cases} \tag{8}$$

2.2. The vertex-interacting self-avoiding walk model

In this section we apply the CTMRG method explicitly to the vertex-interacting self-avoiding walk model introduced by Blöte and Nienhuis [29, 30]. This model consists of a random walk which is allowed to collide at a site, but is not allowed to cross or occupy a bond more than once. An interaction energy $\varepsilon < 0$ is introduced for each collision, which replaces the attractive nearest-neighbour interaction present in the standard Θ-point model. A step fugacity, K, is introduced in order to control the average length of the walk. A stiffness is also introduced by weighting sites sitting on a bend in the walk differently from sites sitting on straight portions of the walk. Following the convention of Blöte and Nienhuis [30], we choose to add a weight p to the straight segments of the walk. The choice $p = 0$ then corresponds to a walk in which straight segments are eliminated (the walk is obliged to turn through a right angle after each step). The partition function for the model is then given by

$$\mathcal{Z} = \sum_{\text{walks}} (Kp)^{N_s} p^{-N_c} \tau^{N_I} \tag{9}$$

where $\tau = \exp(-\beta\varepsilon)$, N_s is the length of the walk (number of steps), N_I is the number of doubly occupied sites and N_c is the number of corners.

2.3. The corner transfer matrix renormalization group method

Following Baxter [31–33], the partition function of a two-dimensional lattice model may be written in terms of the product of four matrices representing the four quarters of the lattice, see figure 2. The inputs and outputs of the matrices are the configurations at the seams of the four quarters. These matrices are known as corner transfer matrices. In general the four

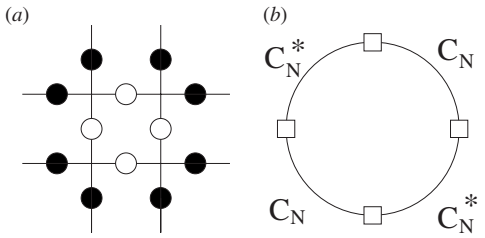

Figure 3. (*a*) The initial vertex lattice. The 3-state spins defined in the vertex model are represented by circles. The black spins are summed over, taking into account the boundary conditions (fixed or free), to give the prototype system used in the CTMRG method, shown in (*b*). The squares represent the *m*-state spins used in the CTMRG method. C_N is an $m \times m$ corner transfer matrix representing one quarter of the lattice (see text). The asterisk represents complex conjugation.

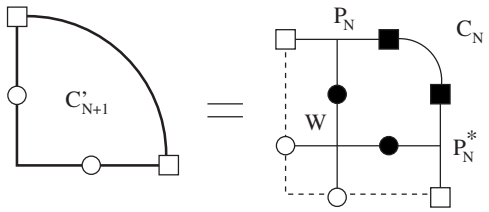

Figure 4. The matrix C'_{N+1} is constructed by adding the vertex functions P_N and W to C_N as shown. The asterisk represents complex conjugation. Circles represent the 3-state spin variables defined by the original model, and the squares represent the *m*-state spins defining the CTMRG prototype system. The black spins are summed over, leaving the white spins as the indices of C'_{N+1}. C'_{N+1} is a $3m \times 3m$ matrix which must then be projected in an optimal way to give the new $(m \times m)$ corner transfer matrix C_{N+1}.

matrices are different, but may often be related by lattice symmetries. For our model the four matrices are the same up to a complex conjugation operation.

In general, it is difficult to explicitly calculate these matrices for systems with a large number of sites. This is where the CTMRG method comes in [18, 24]; the matrices for larger lattices are calculated iteratively from smaller lattices. This is done as follows. A prototype system consisting of a small number of spins, four in the case of a vertex model, is set up exactly, see figure 3. At each iteration the system is enlarged by adding spins, and this enlarged system is then projected back onto the prototype system in some optimal way, so as to minimize the loss of information. The spins of the prototype system have *m* states, where *m* determines the amount of information which may be carried forward at each iteration.

In addition to the vertex function $W(\sigma_i, \sigma_j, \sigma_k, \sigma_l)$, we also introduce the vertex functions $P_N(\sigma_i, \xi_j, \xi_k)$ and $C_N(\xi_i, \xi_j)$ where the ξ_i are the *m*-state spins of the prototype system. The matrix C_N corresponds to the estimate of the corner transfer matrix after *N* iterations. The partition function for a $2N \times 2N$ lattice is given by

$$Z_N = \mathrm{Tr}(C_N C_N^*)^2 \tag{10}$$

where the $*$ denotes complex conjugation. The lattice is enlarged by introducing additional vertices, as shown in figure 4. A corner matrix for the enlarged lattice is given by

$$C'_{N+1} = W \bullet P_N \bullet P_N^* \bullet C_N \tag{11}$$

where $\bullet$ indicates that the appropriate contractions over indices are performed. In a similar way we introduce an enlarged vertex function

$$P'_{N+1} = W \bullet P_N. \tag{12}$$

By considering carefully the symmetry of the vertex function W it may be shown that the partition function for the enlarged lattice $2(N+1) \times 2(N+1)$ is given by

$$Z'_{N+1} = \mathrm{Tr}(C'_{N+1} C'^{*}_{N+1})^2. \tag{13}$$

We now wish to project the enlarged model, defined through C'_{N+1} and P'_{N+1}, back onto the smaller prototype system, giving P_{N+1} and C_{N+1}.

Since the configuration space is smaller after projection, some information is lost. The trick is to minimize this information loss. This is done by performing a change of basis in some optimal manner. The partition function Z'_{N+1} is invariant by any change of basis, but the partial trace, giving Z_{N+1} after the change of basis, is not. For a model with real weights it is clear that the optimal choice will minimize $\varepsilon = |Z'_{N+1} - Z_{N+1}|$. This is done by diagonalizing the matrix $\tilde{z} = (C'_{N+1} C'^{*}_{N+1})^2$ and keeping the basis vectors corresponding to the largest eigenvalues. In a model with real weights $\tilde{z}$ is just the density matrix, up to a constant. In the case considered here the eigenvalues of $\tilde{z}$ are complex, coming in conjugate pairs. Minimizing ε corresponds to taking the basis vectors for the eigenvalues with the largest real parts, since the imaginary parts cancel. This may well involve dropping terms contributing to Z'_{N+1} with larger moduli than other terms which are kept. It is not clear how this effect propagates with the number of iterations. Another choice is to keep the terms contributing to Z'_{N+1} with the largest absolute values. This is found to give better results in practice. To complete the iteration scheme, we must also calculate P_{N+1}. This is done by projecting P'_{N+1} onto P_{N+1} using the same basis vectors. As this iterative process is repeated, the partition function and other thermodynamic quantities are calculated for larger and larger lattices. The value of m defines the size of the configurational space kept from one iteration to the next. The larger the value of m, the better the approximation.

The iteration scheme not only gives an approximation of the partition function for a square system, but also gives an approximation for the transfer matrix from which an infinite strip may be constructed. The transfer matrix is given directly in terms of the vertex functions P_N and W as

$$\mathcal{T} = P_N \bullet W \bullet W \bullet P_N^* \tag{14}$$

for even lattice widths (width $L = 2N + 2$) and

$$\mathcal{T} = P_N \bullet W \bullet P_N^* \tag{15}$$

for odd lattice widths (width $L = 2N+1$). Free energies and correlation lengths for strips may then also be calculated, and the arsenal of finite-size scaling methods available for strips may be used. CTMRG is most efficient, however, when it is used to calculate directly one-point functions, such as the density, and this is how we use it in this paper.

The density is most simply calculated by selecting one of the central lattice bonds. The density ρ is then given by $\rho = \langle |\sigma| \rangle$, where σ is the value of the spin on the selected bond. In terms of the corner transfer matrices,

$$\rho_L = \frac{\mathrm{Tr}(\Lambda C'_N C'^{*}_N C'_N C'^{*}_N)}{\mathrm{Tr}(C'_N C'^{*}_N C'_N C'^{*}_N)} \tag{16}$$

where Λ is a matrix whose elements take the value $|\sigma|$ and $L = 2N$ is the linear dimension of the lattice.

In spin models the one-point functions are often calculated by the infinite lattice method [24], where the CTMRG method is iterated for a fixed value of m until the quantity of interest (magnetization or energy per spin) no longer changes. This occurs because the number of eigenstates kept at each iteration is no longer sufficient to propagate the two-point correlations

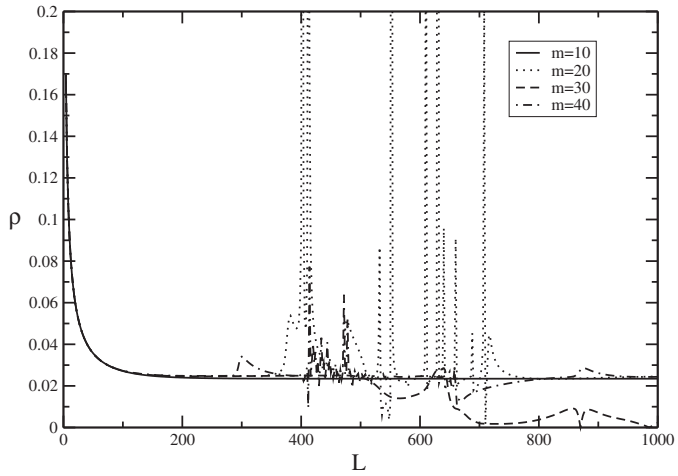

Figure 5. Variation of the density ρ for the self-avoiding walk model ($p = 1, \tau = 0$) calculated using CTMRG as a function of the linear size $L = 2N$ of the lattice for different values of m.

throughout the system. The limiting value of the one-point correlation function may then be studied as a function of m. In such a manner the magnetization or energy per site may be estimated for the infinite system directly. This method relies on the rather nice way in which CTMRG breaks down for spin models. Unfortunately, the complex nature of the vertex models at the heart of our calculations gives rise to more complicated behaviour as m is increased. Figure 5 shows the density of the self-avoiding walk model ($p = 1, \tau = 0$ and $n = 0$, or equivalently $\theta = \pi/2$) as a function of L for different values of m. It is clearly seen that there is no limiting value for the density as L is increased. Once the value of m is insufficient, ρ has a chaotic oscillatory behaviour with L. Instead of fixing m and varying L, we choose to do the opposite. Taking the density as an example, we define $\rho_L(m)$ as the density for a system of linear dimension L for a given value of m. The limiting value of $\rho_L(m)$ is calculated by increasing the value of m for fixed L until the required accuracy for ρ_L is reached. This is then studied as a function of L using finite-size scaling methods, described below.

3. Results

3.1. The vertex-interacting model with $p = 0$

When $p = 0$ the model is expected to have a critical behaviour equivalent to the standard Θ-point model [16]; for small enough τ the average length of the walk diverges as a critical value of the step fugacity, K_c, is reached. At K_c the density is still zero and the gyration radius, R_G, (or any other characteristic measure of the size of the walk) diverges as $K \to K_c^-$ following a power law defining the correlation length exponent ν:

$$\xi \sim (K_c - K)^{-\nu}. \tag{17}$$

For τ smaller than some tricritical value, τ_{tc}, the walk is in the same universality class as the usual self-avoiding walk, and $\nu = 3/4$. This behaviour terminates at the tricritical point (K_{tc}, τ_{tc}), where $\nu = 4/7$ as for the standard Θ point. For values of $\tau > \tau_{tc}$ the length of the walk diverges discontinuously at a first-order transition. The phase diagram of the $p = 0$ vertex-interacting model is qualitatively the same as for the Θ point [16] and is shown

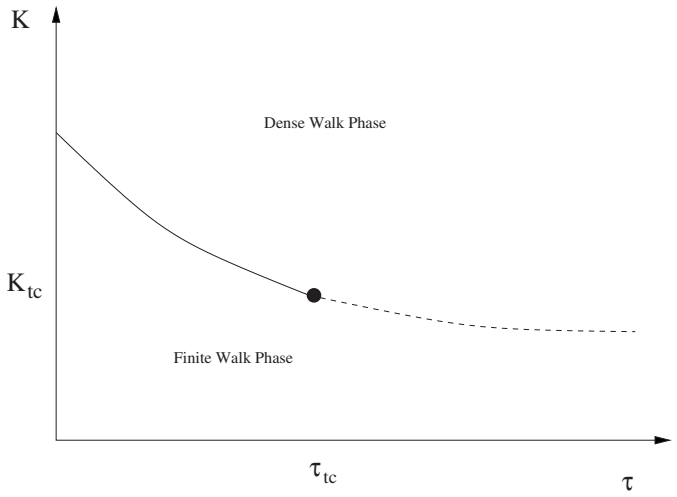

Figure 6. The schematic phase diagram for the vertex-interacting model with $p = 0$. For $p = 0$ the vertex-interacting model has the same schematic phase diagram as the Θ-point model, and the same critical behaviour. The solid line corresponds to a critical phase transition in the self-avoiding walk universality class. The dashed line corresponds to a first-order transition. The two types of phase transition are separated by a tricritical point ($K_{tc} = 1/2$, $\tau_{tc} = 2$).

schematically in figure 6. Unlike for the standard Θ-point model, the location of the tricritical point is known exactly to be ($K_{tc} = 1/2$, $\tau_{tc} = 2$) [16].

The idea is now to study this model using the CTMRG method outlined. As mentioned in section 2.3, CTMRG gives as a by-product an approximation of the transfer matrix for a strip of width L through (14) or (15), depending on the parity of L, from which the phase diagram and critical exponent ν could be calculated using the phenomenological renormalization group due to Nightingale [20]. This turns out, at least for the case at hand, not to be the most efficient way of approaching the problem, due to the additional computational effort required to calculate the relevant eigenvalues of $\mathcal{T}$. The CTMRG method is far more efficient for the calculation of one-point functions, such as the bond density, which may be calculated in the middle of the system. With this in mind we use a phenomenological renormalization scheme based directly on the scaling behaviour of density.

The scaling ansatz states that the singular part of the free energy is a homogeneous function of its arguments [34]. This leads to the following finite-size scaling expression:

$$f_s(K, L) = L^{-d} \tilde{f}(|K - K_c| L^{1/\nu}) \tag{18}$$

where d is the spatial dimension, here $d = 2$. Taking the first derivative,

$$\rho_s(K, L) = L^{1/\nu - 2} \tilde{\rho}(|K - K_c| L^{1/\nu}). \tag{19}$$

In general

$$\rho(K, L) = \rho_\infty(K) + \rho_s(K, L) \tag{20}$$

and so it is necessary to know the value of $\rho_\infty(K)$ in order to exploit fully the scaling behaviour. The density of a finite walk on an infinite lattice is zero, and so $\rho_\infty(K < K_c) = 0$. This enables the setting up of a phenomenological renormalization group method using the function

$$\varphi_{L,L'}(K) = \frac{\log(\rho_s(K, L)/\rho_s(K, L'))}{\log(L/L')}. \tag{21}$$

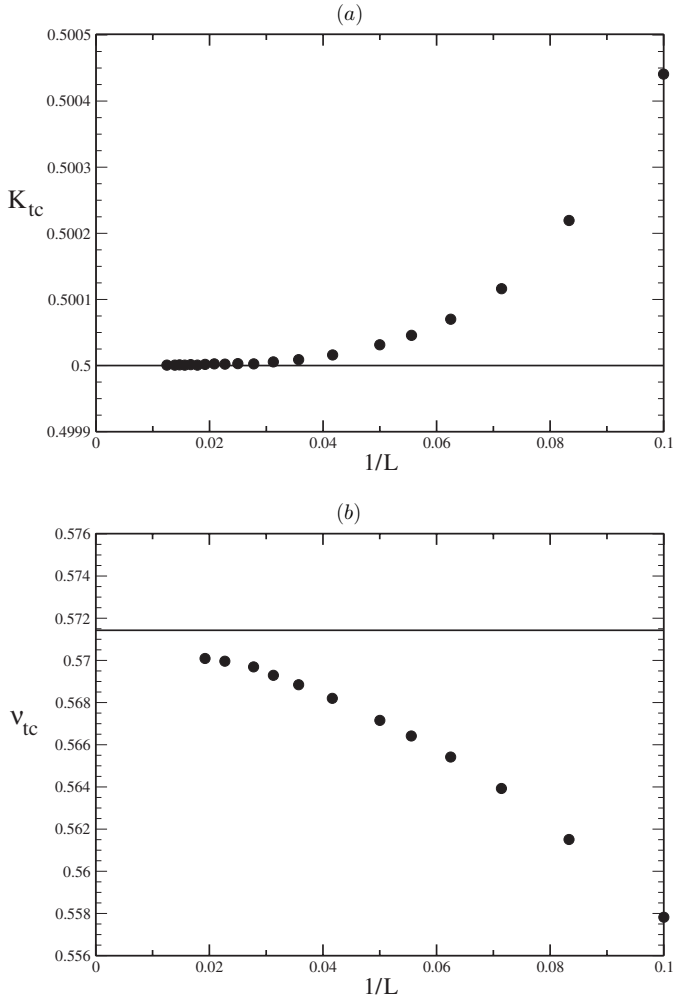

Figure 7. Estimates of the tricritical values K_{tc} and ν_{tc} calculated for $p = 0$ and $\tau = \tau_{tc} = 2$ using (22), plotted as a function of the linear size L. There is a clear convergence to the expected exact values $K_{tc} = 1/2$ and $\nu_{tc} = \nu_\theta = 4/7$.

Using (19) we find that $\varphi_{L,L'} = 1/\nu - 2$ independently of L and L'. Naturally there are additional finite-size corrections which should be taken into account, but the conclusion is that if the function $\varphi_{L,L'}(K)$ is plotted for various values of L and L' then it will converge to a fixed point given by $\varphi(K_c) = 1/\nu - 2$. In what follows we have set $L' = L - 2$ and looked for solutions of the equation

$$\varphi_{L,L-2}\big(K_c^L\big) = \varphi_{L-2,L-4}\big(K_c^L\big). \tag{22}$$

If such solutions exist then $K_c = \lim_{L\to\infty} K_c^L$ and $\nu = \lim_{L\to\infty} 1\big/\big(2 + \varphi_{L,L-2}\big(K_c^L\big)\big)$.

Preliminary results using CTMRG were recently reported in [18]; notably the density profiles and values for K_c and ν are given for various values of τ with $p = 0$. When $p = 0$, the vertex-interacting Θ point is known to occur exactly at $K_{tc} = 1/2$ and $\tau_{tc} = 2$. In figure 7 we present results using this scheme where we have fixed $p = 0$ and $\tau = \tau_{tc} = 2$. The results converge rather quickly to the exact values, $K_c = 1/2$ and $\nu_\Theta = 4/7$. Whilst

here the tricritical values of K, τ and ν are known exactly, this is in general not the case. It is interesting to know how well the method works with no external input. As we pass through τ_{tc} the value of ν changes from $\nu_{\mathrm{SAW}} = 3/4$ for $\tau < \tau_{tc}$ to $\nu_\Theta = 4/7$ for $\tau = \tau_{tc}$ and on to $\nu = 1/2$ for $\tau > \tau_{tc}$. This last value is simply a reflection of the fact that the density is nonzero, and so $R_G \sim N^{1/2}$. Clearly the finite-size estimates, $\nu_L(\tau)$, will be continuous functions of τ, tending to the step function only in the infinite lattice limit. If the different $\nu_L(\tau)$ cross, then these intersections necessarily tend, in the limit of an infinite system, to the correct values: $\nu_{tc} = \nu_\theta$ and τ_{tc}. This is a standard method used to determine numerically the location, for example, of the Θ point in the standard model (see for example [7–9]). The estimates derived from this method are shown in figure 8 plotted as a function of $1/L$. The estimates converge convincingly to the exact values $\tau_{tc} = 2$, $K_{tc} = 1/2$ and $\nu_{tc} = 4/7$.

3.2. The vertex-interacting model with $p = 1$

What is interesting about the vertex-interacting model is that the phase diagram is very different when $p \neq 0$ [35]. Naïvely one would expect the $p = 1$ model to also be equivalent to the Θ-point model; the model consists of a walk which is essentially self-avoiding with short-ranged attractive interactions. This is in fact not the case; an additional transition arises in the dense-walk phase and the nature of the transition at the (now) multicritical point changes. There are no exact results for the location of the multicritical point (K_{mc}, τ_{mc}) as was the case for $p = 0$. There exist, however, exact predictions for the universality classes of the different phase transitions. The low-density phase transition is expected to be in the self-avoiding walk universality class (with $\nu = 3/4$) [30, 35]. The high-density critical line is expected to be in the Ising universality class ($\nu = 1$) [30, 35]. The value of ν_{mc} at the multicritical point has been found from an exact result for the 19 vertex model with complex weights used in our calculations. It is predicted that $\nu_{mc} = 12/23$ [19]. In the remainder of this section we calculate the phase diagram and compare critical exponent estimates calculated from the CTMRG method with the known results.

In figure 9 the density is plotted as a function of K for $p = 1$ and $\tau = 1$. The presence of two phase transitions may clearly be seen, the first between the zero-density phase and a dense-walk phase, and the second between two dense-walk phases.

For the first transition, as K is increased, it is possible to use the scaling arguments given in section 3.1 since the density in the thermodynamic limit is zero. For the second transition, however, the density is nonzero, and *a priori* unknown. To apply the scaling arguments it is necessary to estimate the density in the infinite lattice limit, $\rho_\infty(K)$. Alternatively it is possible to eliminate ρ_∞ by using two lattice sizes. Along with (19) and (20) this gives a new finite-size scaling function

$$\tilde{\varphi}_L(K) = \frac{\log\left(\frac{\rho(K,L)-\rho(K,L-2)}{\rho(K,L-2)-\rho(K,L-4)}\right)}{\log\left(\frac{L}{L-2}\right)} \tag{23}$$

which, as before, may be used to find estimates of the critical lines by looking for solutions of the equation

$$\tilde{\varphi}_L\left(K_c^L\right) = \tilde{\varphi}_{L-2}\left(K_c^L\right). \tag{24}$$

In the limit $L \to \infty$ the solutions of this equation tend to the correct fixed points, such that $\tilde{\varphi}\left(K_c^L\right) \to 1/\nu - 3$. This again enables the calculation of the critical exponent ν.

The high-density transition line is expected to be in the Ising universality class, with an exponent $\nu = 1$. It is important to note that the exponent is used to represent both the critical exponent related to the correlation length and the inverse of the Haussdorf dimension, d_H [36].

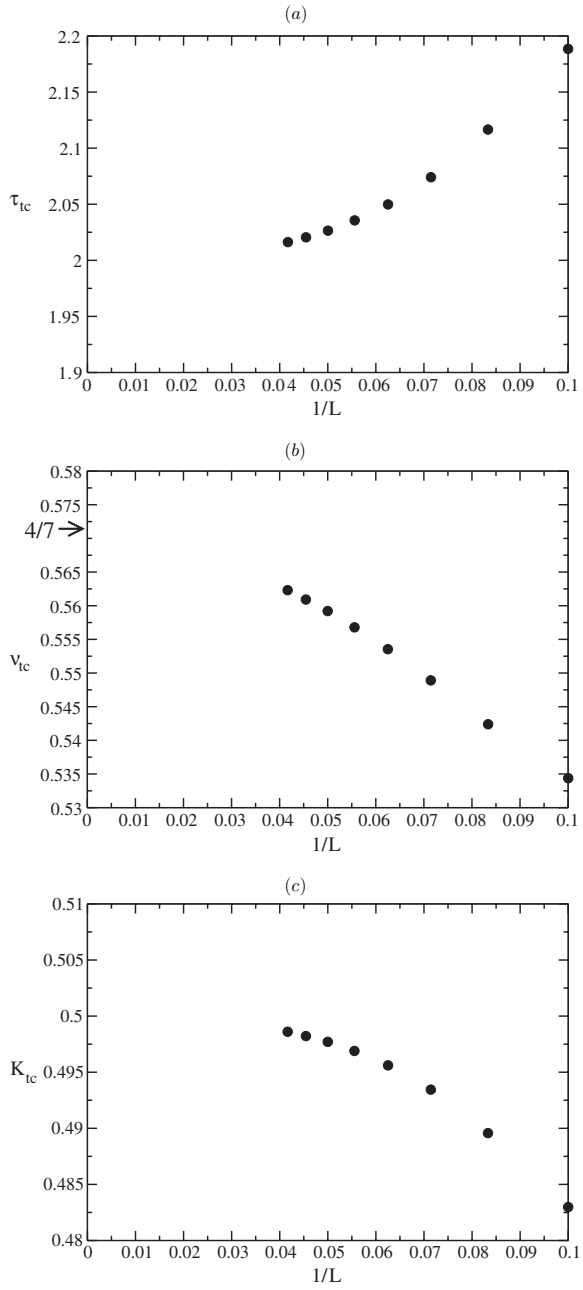

Figure 8. Estimates of the tricritical values (*a*) τ_{tc}, (*b*) ν_{tc} and (*c*) K_{tc} calculated from the intersections of $\nu_L(\tau)$ for $p = 0$. There is a clear convergence to the exact values $\tau_{tc} = 2$, $\nu_{tc} = 4/7$ and $K_{tc} = 1/2$.

The Haussdorf dimension is the fractal dimension defined through the scaling of the density with the distance from the centre of mass of the walk. This leads to the scaling law:

$$R_G \sim N^{1/d_H} \tag{25}$$

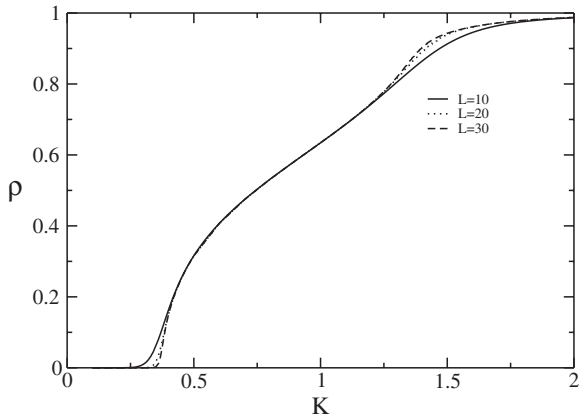

Figure 9. The density of the walk on the lattice for $p = 1$ and $\tau = 1$ as a function of K, clearly showing the existence of two phase transitions.

where R_G is the radius of gyration, or any other characteristic measure of the linear size of the walk. Since in the low density regime the gyration radius is proportional to the correlation length, then as the critical line is approached, and $L \to \infty$, we may identify $\nu = 1/d_H$. It is common practice to define ν from (25), whence $\nu = 1/d = 1/2$ on the first-order transition line, where the fractal and space dimensions become the same. The ν associated with the high-density transition will necessarily not be defined in this geometrical fashion, but corresponds to the true thermodynamic critical exponent related to the correlation length. The estimate of K_c and the associated estimates for ν are given in figure 10 for $p = 1$ and $\tau = 1$. The evolution of ν is not monotonic, emphasizing the need to go to large enough lattice sizes before having reliable estimates of the exponent. It is clear that ν converges to the expected value $\nu = 1$, and we estimate the critical fugacity in this case to be $K_c = 1.326 \pm 0.002$.

Figure 11(a) shows the phase diagram where both transition lines are calculated using the scaling function given in (23). In practice there are usually two solutions to (23) corresponding to the same transition; both converge towards the same value of K_c as the size of the lattice is increased. However, one of these solutions evolves more slowly than the other as system size is increased, and this is taken as being the relevant solution for the calculation of ν and K_c. As τ is increased these two solutions come closer (for fixed lattice size), and join at a certain value of τ. Beyond this value of τ there is no longer a solution corresponding to the transition in question (there may be solutions corresponding to other transitions). This vanishing point moves to larger τ as the lattice size is increased. The phase diagram shown in figure 11(a) is calculated for system sizes up to $L = 30$.

Figure 11(b) shows the estimates for the zero-density phase transition lines calculated using (21). As τ approaches its multicritical value, the finite-sized system feels the presence of the high-density phase transition, leading to a peak in the estimated transition line. This peak reduces in size rapidly as the system size is increased.

Estimates of the location of the multicritical point, (K_{mc}, τ_{mc}), may again be found by looking for crossings in the finite-size estimates of $\nu(\tau)$ calculated along the self-avoiding walk transition line using (21) and (22). These estimates are given in figure 12. The location of the multicritical point is estimated as $K_{mc} = 0.3408 \pm 0.0002$, $\tau_{mc} = 4.69 \pm 0.01$. These estimates agree very well with the estimates given by Guo *et al* [35], who give $z_{mc} = K_{mc}^2 \tau_{mc} \approx 0.54$,

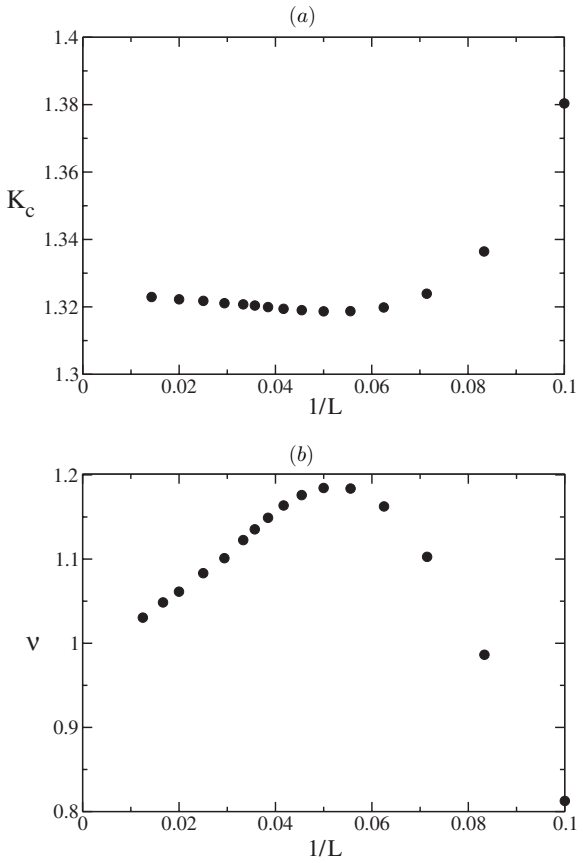

Figure 10. Estimates of K_c and ν corresponding to the high-density phase transition plotted as a function of $1/L$ for $p = 1$ and $\tau = 1$. The estimated value of $K_c = 1.326 \pm 0.002$ and convergence to the expected value of $\nu = 1$ is observed.

however the finite-size estimates of $\nu_L(\tau)$ cross at a value too low to be consistent with the exact value at the multicritical point ($\nu_{L\to\infty} \approx 0.51$ compared with $\nu_{\text{exact}} = 12/23 = 0.5217\ldots$). This leads to the conclusion that either the scaling method is flawed or $\rho_\infty \neq 0$ at the multicritical point. In figure 13 the density is plotted as a function of τ along the critical (self-avoiding walk) line. At the multicritical point the density has a clear finite limit as the size is increased, indicating that the transition is first order as approached in this direction. As further evidence of the first-order character of the transition when approached following the self-avoiding walk line we plot in figure 14 the finite-size estimates of K_c and ρ for different values of τ near τ_{mc}. From figure 11 it is seen that for τ close to τ_{mc} the system is influenced by the high-density transition. As the system size is increased, the estimates transit to the zone of influence of the zero-density transition, where they tend to their limiting values. This transit is clearly seen in figure 14 for $\tau = 4.3 < \tau_{mc}$. When $\tau = 4.6$ it is seen that the transit begins, but the sizes we could consider in a practical time scale were not large enough to see the end of the transition. It is however reasonable to suppose that for $\tau = 4.6$ the limiting density will be zero and occur as $L \to \infty$. No such transit is seen for $\tau = 4.7 > \tau_{mc}$, which displays a nonzero limiting density. The precise value of this limiting density is of course not reliable, since the location of the transition point, found assuming $\rho_\infty = 0$, will

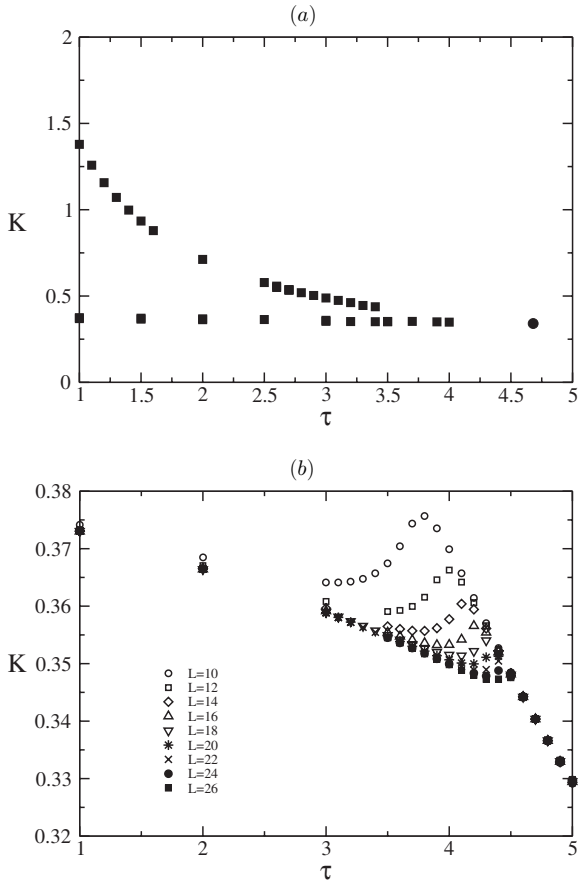

Figure 11. The phase diagram calculated using (*a*) 23 with $L = 30$ and (*b*) 21, having fixed $\rho_\infty = 0$, plotted for different values of L between 10 and 26. In (*a*) solutions corresponding to the low- and high-density phase transitions are shown, while in (*b*) only the low-density transition was obtained. The circle in (*a*) shows the numerically estimated location of the multicritical point (see text and figure 12).

not be precise. The determination of the multicritical point is however expected to be correct since $\rho_\infty = 0$ along the entire self-avoiding walk line, as must be the case since the fractal dimension $d_H = 1/\nu < 2$.

There exist five branches of solutions for the Blöte–Nienhuis $O(n)$ model on the square lattice [30], through its mapping onto the 19 vertex model, for which the (multi)critical points are exactly known, as well as many of the critical exponents. The multicritical point here is thought to correspond to the same universality class as the $n = 0$ solution belonging to the third branch. The location of this point is given exactly as [30]:

$$\left.\begin{aligned} z = K^2\tau &= \left\{2 - [1 - 2\sin(\theta/2)]\,[1 + 2\sin(\theta/2)]^2\right\}^{-1} \\ K &= -4z\sin(\theta/2)\cos(\pi/4 - \theta/4) \\ pK &= z\,[1 + 2\sin(\theta/2)] \\ \theta &= -\pi/4 \end{aligned}\right\}. \tag{26}$$

This gives the location of the exactly known multicritical point as $K^*_{mc} = 0.446933\ldots$, $p^*_{mc} = 0.275899\ldots$ and $\tau^*_{mc} = 2.630986\ldots$. We checked the determination of this point using

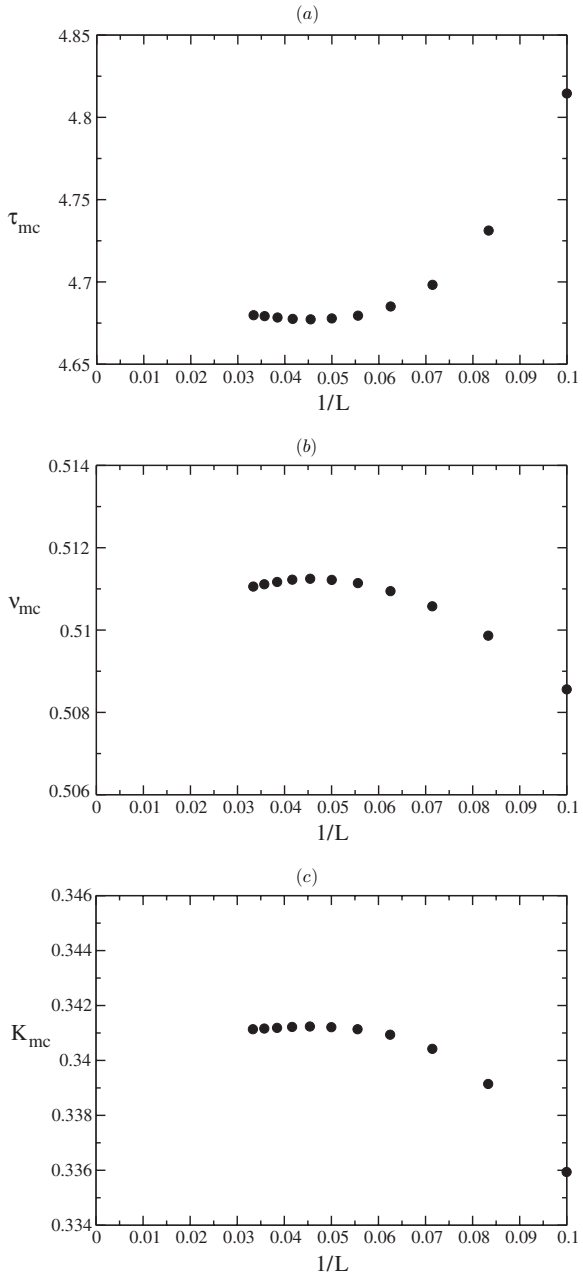

Figure 12. Estimates of (*a*) τ_{mc}, (*b*) ν_{mc} and (*c*) K_{mc} calculated from the intersections of $\nu_L(\tau)$ for the vertex-interacting model with $p = 1$ and fixing $\rho_\infty = 0$. The estimated position of the multicritical point is then found to be $K_{mc} = 0.3408 \pm 0.0002$ and $\tau_{mc} = 4.69 \pm 0.01$. The estimated value of ν_{mc} is incompatible with the exact value $\nu_{mc} = 12/23 \approx 0.5217$ for reasons explained in the text.

CTMRG fixing $p = p^*_{mc}$ and $\tau = \tau^*_{mc}$ and looking for the limiting value of K_L. This is shown in figure 15 and is clearly consistent with the exact known value. The density was then

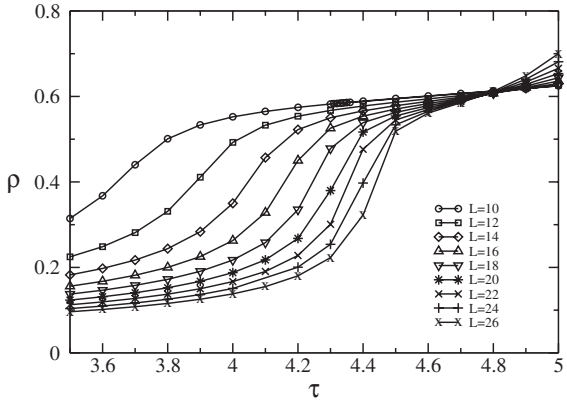

Figure 13. The density plotted as a function of τ calculated along the critical self-avoiding walk line $K_c(\tau)$. The density appears to be developing a jump at around τ_{mc} as the system size, L, is increased.

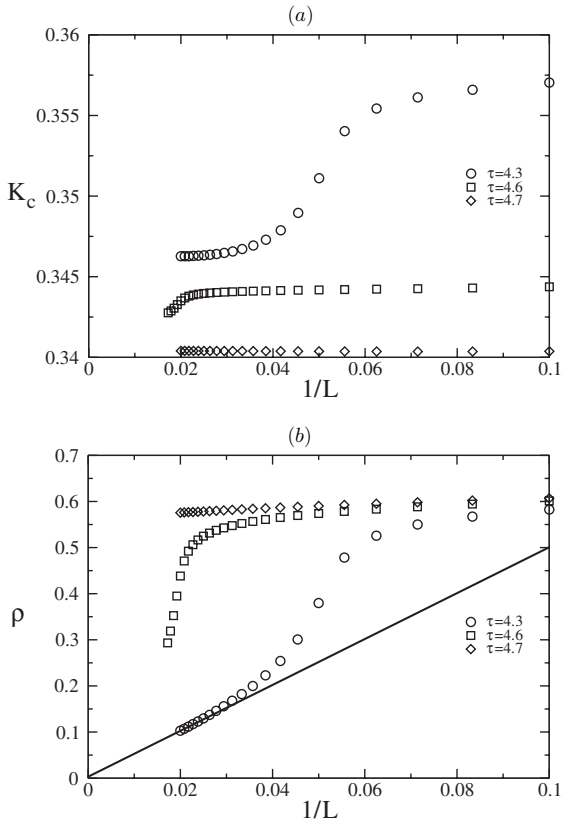

Figure 14. (*a*) The estimates of K_c and (*b*) estimates of the density plotted as a function of $1/L$ for three values of τ: $\tau = 4.3$ and $\tau = 4.6$ which are below τ_{mc} and $\tau = 4.7$ which is above τ_{mc}. When $\tau < \tau_{mc}$ the graphs show a transit from being influenced by the high-density transition line (small L) to being influenced by the zero-density transition line (large L). Whilst the transit is not complete for the sizes considered when $\tau = 4.6$, it is clear that $\rho_\infty = 0$ in this case whilst $\rho_\infty \neq 0$ when $\tau = 4.7$. The solid line is given as a guide to the eye.

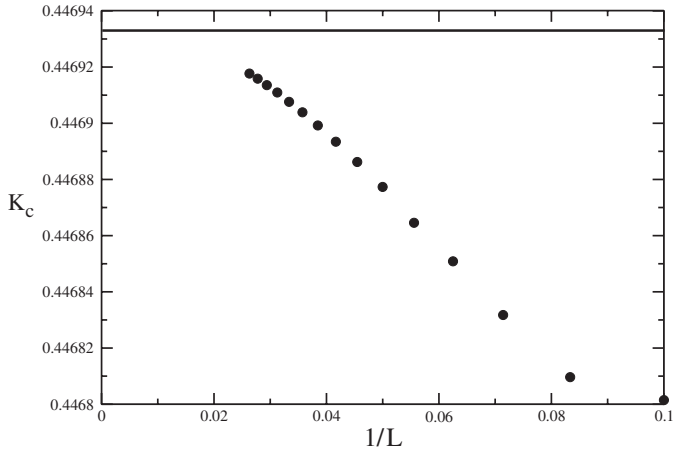

Figure 15. Estimates of K_c calculated using (21) with $p = p^*_{mc}$ and $\tau = \tau^*_{mc}$ fixed at the values given by the exact solution (26). The estimates converge well to the exact value $K^*_{mc} = 0.446933\ldots$ (shown by the solid line) as $L \to \infty$.

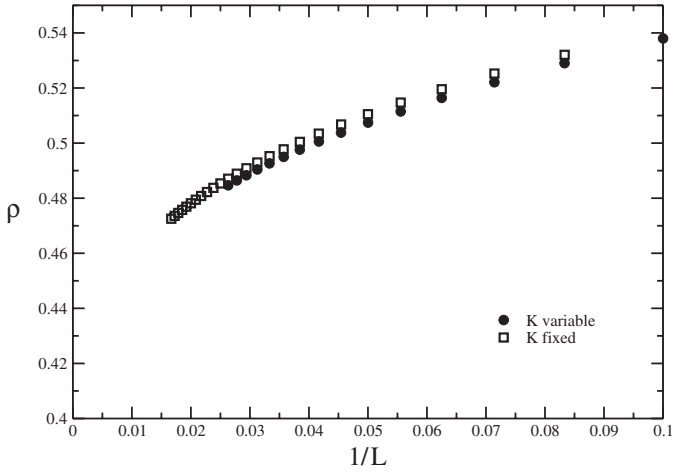

Figure 16. The density plotted for (*a*) $p = p^*_{mc}$ and $\tau = \tau^*_{mc}$ given by the exact solution (26) whilst K_{mc} is calculated from (21) (filled circles) and (*b*) p, τ and K fixed by (26) (squares). The density does not become zero in the limit $L \to \infty$. A conservative estimate of the limiting density would be 0.43 ± 0.01.

calculated firstly at the finite-size estimate of the critical point and then fixing simultaneously the values of K, p and τ to the values given in (26) (see figure 16). In both cases a conservative estimate gives $\rho_\infty = 0.43 \pm 0.01$. These results indicate that the 'multicritical' point is fairly exotic in that it corresponds generically to a first-order transition but with a critical behaviour if approached in a specific direction. We have tried to recover the critical exponent $12/23$ by using the scaling behaviour of the density at K^*_{mc}, τ^*_{mc} and p^*_{mc}. Whilst the results are not inconsistent with $\nu = 12/23$, they are not of very good quality and are also not inconsistent with a value $\nu \approx 0.54$ as originally found by Blöte and Nienhuis using transfer matrices [30].

Whilst in principle there is no limit to either the precision or lattice sizes obtainable using CTMRG, there is a practical limitation in terms of computing time and resources.

4. Conclusion

In this paper we have presented a version of the corner transfer matrix renormalization group method suitable for use with self-avoiding walk-type models and related $O(n)$ symmetric models. We have applied it to the vertex-interacting self-avoiding walk model. The method was shown to reproduce the known results and has given new insight into the critical nature of the model when $p \neq 0$.

Self-avoiding walk models are used as models for polymers in dilute solution, and it is known that the lattice θ-point model provides a good description of what happens for real homopolymers in solution [1]. The standard textbook reason for not taking into account the rigidity of the polymer is that the rigidity simply changes the persistence length, or in terms of the lattice model the number of real monomers per step of the walk. The critical behaviour is unaffected in the infinite walk limit. This should be true as long as the fractal dimension d_H is smaller than the spatial dimension (i.e. $d_H < 2$ here). However, when $d_H = d$ it may be expected that the polymer feels the presence of the lattice. This will then give rise to competition between the rigidity and the underlying lattice structure, reminiscent of frustration in spin models (indeed the critical behaviour of the Nienhuis $O(n)$ model on the square lattice has been related to the fully frustrated XY model [30]). If such a claim is true, then the critical behaviour observed will be universal (in the sense of not depending on the lattice) and independent of rigidity if $d_H < d$, and may be non-universal (in the same restricted sense) and may depend on the rigidity if $d_H = d$. One could therefore argue that the simple observation that the critical behaviour of the collapse transition changes as p is varied implies that the density is nonzero at the collapse transition when $p \neq 0$. In interpreting this transition as due to frustration, it should be noted that it does not exist for the $O(n)$ model on the hexagonal lattice [26, 27].

There are other models which have qualitatively similar phase diagrams. Most well known is the self-avoiding trail model [37]. A trail is defined to be self-avoiding on the bonds, but is allowed to visit sites more than once, and in particular is allowed to intersect itself. The attractive interaction is again associated with doubly visited sites (intersection or collision). It has been conjectured that the collapse transition for trails occurs exactly at $\tau = 3$ with an exponent $\nu = 1/2$; it is also conjectured that limiting density is zero. This conjecture resulted from a Monte Carlo enumeration of extremely long walks of the kinetic trail model, believed to be equivalent to the trail model at the collapse transition [38] . As discussed above, in this case what is being calculated is in fact the fractal dimension d_H. The relation $\nu = 1/d_H$ is only valid when the critical length may be measured using the gyration radius. As argued above, the validity of this identification may be questioned when $d_H = d$. It would be of interest, then, to check by other means the possibility that the criticality is in fact not of the same type as observed here for $p \neq 0$. This question is currently under investigation.

Another model with a qualitatively similar phase diagram is the hydrogen-bonding model [17]. This model includes interactions between nearest-neighbour sites, which may be taken into account in the CTMRG method by mapping the walk model onto a 4-state vertex model with complex weights. There are, however, important differences, notably the high-τ dense-walk phase has $\rho \equiv 1$ throughout, whereas here $\rho \neq 1$ except in the limit $\tau \to \infty$. To what extent this may affect the nature of the phase transitions is not clear; early results indicate that perhaps the dense-walk phase transition is not in the Ising universality class [39].

References

[1] de Gennes P G 1979 *Scaling Concepts in Polymer Physics* (Ithaca: Cornell University Press)
Vanderzande C 1998 *Lattice Models of Polymers* (Cambridge: Cambridge University Press)
des Cloiseaux J and Jannink G 1990 *Polymers in Solution: Their Modelling and Structure* (Oxford: Oxford University Press)
[2] de Gennes P G 1972 *Phys. Lett.* A **38** 339
[3] Landau D P and Binder K 2000 *Monte Carlo Simulations in Statistical Physics* (Cambridge: Cambridge University Press)
[4] Gaunt D S and Guttmann A J 1974 *Phase Transitions and Critical Phenomena* vol 3, ed C Domb and M S Green (London: Academic)
Guttmann A J 1989 *Phase Transitions and Critical Phenomena* vol 13, ed C Domb and J Lebowitz (New York: Academic)
[5] Klein D G 1980 *J. Stat. Phys.* **23** 561
[6] Enting I G 1980 *J. Phys. A: Math. Gen.* **13** 3713
[7] Derrida B 1981 *J. Phys. A: Math. Gen.* **14** L5
[8] Derrida B and Herrmann H G 1983 *J. Physique* **44** 1365
[9] Derrida B and Saleur H 1985 *J. Phys. A: Math. Gen.* **18** 1075
[10] Veal A R, Yeomans J M and Jug G 1991 *J. Phys. A: Math. Gen.* **24** 827
[11] Binder K 1994 *Advances in Polymer Science* vol 112 (Berlin: Springer)
[12] Caracciolo S, Causo M S, Grassberger P and Pelissetto A 1999 *J. Phys. A: Math. Gen.* **32** 2931
Frauenkron H, Bastolla U, Gerstner E, Grassberger P and Nadler W 1998 *Phys. Rev. Lett.* **80** 3149
Grassberger P, Hegger R and Schäfer L 1994 *J. Phys. A: Math. Gen.* **27** 7262
Grassberger P and Hegger R 1996 *J. Phys. A: Math. Gen.* **29** 279
Grassberger P 1997 *Phys. Rev.* E **56** 3682
[13] Tesi M C, van-Rensburg E J J, Orlandini E and Whittington S G 1996 *J. Stat. Phys.* **82** 155
[14] Jensen I and Guttmann A J 1999 *J. Phys. A: Math. Gen.* **32** 4867
[15] Foster D P, Orlandini E and Tesi M C 1992 *J. Phys. A: Math. Gen.* **25** L1211
[16] Blöte H W J, Batchelor M T and Nienhuis B 1998 *Physica* A **251** 95
[17] Foster D P and Seno F 2001 *J. Phys. A: Math. Gen.* **34** 9939
[18] Foster D P and Pinettes C 2003 *Phys. Rev.* E **67** 045105(R)
[19] Warnaar S O, Batchelor M T and Nienhuis B 1992 *J. Phys. A: Math. Gen.* **25** 3077
[20] Nightingale M P 1976 *Physica* A **83** 561
[21] Henkel M and Schütz G 1988 *J. Phys. A: Math. Gen.* **21** 2617
[22] White S R 1992 *Phys. Rev. Lett.* **69** 2863
White S R *Phys. Rev.* B **48** 10345
[23] Peschel I, Wang X, Kaulke M and Hallberg K 1999 *Density-Matrix Renomalization (Lecture Notes in Physics)* (Berlin: Springer)
[24] Nishino T and Okunishi K 1996 *J. Phys. Soc. Japan* **65** 891
Nishino T and Okunishi K 1997 *J. Phys. Soc. Japan* **66** 3040
[25] See for example: Yeomans J M 1992 *Statistical Mechanics of Phase Transitions* (Oxford: Oxford University Press) ch 5
[26] Nienhuis B 1982 *Phys. Rev. Lett.* **49** 1062
[27] Nienhuis B 1987 *Phase Transitions and Critical Phenomena* vol 11, ed C Domb and J L Lebowitz (London: Academic)
[28] Baxter R J 1986 *J. Phys. A: Math. Gen.* **19** 2821
[29] Nienhuis B 1990 *Int. J. Mod. Phys.* B **4** 929
[30] Blöte H W J and Nienhuis B 1989 *J. Phys. A: Math. Gen.* **22** 1415
[31] Baxter R J 1968 *J. Math. Phys.* **9** 650
[32] Baxter R J 1978 *J. Stat. Phys.* **19** 461
[33] Baxter R J 1982 *Exactly Solved Models in Statistical Mechanics* (New York: Academic)
[34] Stanley H E 1971 *Introduction to Phase Transitions and Critical Phenomena* (Oxford: Oxford University Press)
[35] Guo W, Blöte H W J and Nienhuis B 1999 *Int. J. of Mod. Phys.* C **10** 301
[36] Mandelbrot B B 1984 *The Fractal Geometry of Nature* (San Francisco: Freeman)
[37] Malakis A 1976 *Physica* **84** 256
Shapir Y and Oono Y 1984 *J. Phys. A: Math. Gen.* **17** L39
[38] Owczarek A L and Prellberg T 1995 *J. Stat. Phys.* **79** 951
[39] Foster D P and Pinettes C 2003 in preparation